Coupled Systems Mechanics, *Vol. 15, No. 1 (2026) 83-100*
https://doi.org/10.12989/csm.2026.15.1.083

Techno-Press

Study of frequency influence on transversely isotropic thermoelastic diffusive solid under MGT model

Heena*, Parveen Lata

Department of Mathematics, Punjabi University, Patiala, Punjab, India

(Received December 7, 2025, Revised February 202026, Accepted February 232026)

Abstract. This research deals with deformation of a two-dimensional homogeneous transversely isotropic thermoelastic-diffusive solid under chemical potential and thermal loads within the framework of Moore-Gibson-Thompson (MGT) thermoelasticity with two temperatures. Fourier transformation is used to solve the problem and then numerical inversion technique is applied to obtain the solution in physical domain. The application of a time harmonic concentrated and distributed loads are considered to show the utility of the obtained solution. Graphical representation of variation in the stress components, conductive temperature and chemical potential with distance is depicted by taking the effect of frequency.

Keywords: chemical potential; frequency domain; Moore-Gibson-Thompson model; thermoelastic diffusion

1. Introduction

The study of thermomechanical interactions in elastic bodies has become great interest of researchers due to its wide applicability in various physical problems. The coupled theory of thermoelasticity proposed by Biot [1] overcomes the drawbacks of coupled formulation; however it still shares the same flaw of predicting an infinite speed for thermal speed propagation.

To eliminate this flaw, Lord and Shulman [2] formulated the first generalized thermoelastic theory by incorporating a single relaxation time into Fourier's law of heat conduction. Green and Lindsay [3] extended this approach by incorporating two-relaxation times. Later, Green and Naghdi [4-6] introduced three theories of thermoelasticity: the GN-I theory, equivalent to the classical coupled model; the non-dissipative GN-II theory; and the GN-III theory, which includes energy dissipation and predicts damped thermal waves. Further modifications involving additional relaxation parameters led to the dual-phase lag model of Tzou [7] and the three-phase lag model of Choudhary [8].

Although GN-III theory improves on earlier theories, it still predicts the instantaneous heat transfer, similar to Fourier' s law, and therefore can not describe the steady-state behavior. To overcome this drawback, Moore-Gibson-Thompson (MGT) theory was developed. Thompson [9] first formulated the MGT equation for fluid flow, and Dell' Oro and Pata [10] explored its relationship with linear viscoelasticity. Quintanilla [11] later introduced the MGT model into

*Corresponding author, Ph.D. Student, E-mail: heena_rs@pbi.ac.in

ISSN: 2234-2184 (Print), 2234-2192 (Online)

thermoelasticity and also proposed a two-temperature heat conduction model [12]. Owing to its enhanced transient stability, the MGT model has been applied to acoustic materials and various non-classical diffusion scenarios.

Similar to the advancement of heat conduction theories, the understanding of mass diffusion in thermoelastic materials has evolved over time. The growing application of thermoelastic diffusion theory in areas such as solid-state physics, oil extraction techniques, material science, and geophysical studies has stimulated significant interest and research activity in this area. Diffusion refers to the movement of particles within a medium from region of higher concentration to that of lower concentration until equilibrium is reached. The earliest thermoelastic diffusion model was proposed by Nowacki [13-15] using Fick's law, which inherently predicts an infinite speed for diffusion waves. Sherief et al. [16] subsequently proposed a generalized model that allows diffusion waves to propagate at finite speed.

Sharma et al. [17] studied the dynamical behavior of generalized thermoelastic diffusion problem with two-relaxation times in frequency domain. The thermoelastic response of a transversely isotropic half-space influenced by mass-diffusion was studied by Abbas et al. [18]. The state of plane strain problem parallel to xz −plane in the discipline of thermoelasticity is discussed by Abbas and Othman [19] and Kumar et al. [20]. Zenkour [21] also studied two-temperature problem for anisotropic plate containing a circular cavity with two relaxation times. Abbas and Abo-Dahab [22] also estimated the influence of relaxation times for generalized magneto-thermoelastic theory. Abouelregal and Sedighi [23] investigated one-dimensional half space subjected to chemical potential and thermal shock within the framework of MGT thermodiffusion theory. Sur [24] considered MGT generalized heat conduction theory to discuss the comparison between isotropic and transversely isotropic material. Abouelregal et al. [25, 26] studied the modified MGT heat transfer model with memory dependent derivatives to investigate the thermoelastic interactions. Singh and Lata [27] and Gerba et al. [28] studied the frequency effect within the nonlocal theory of thermoelasticity. Adel et al. [29] considered isotropic medium to discuss the response of thermoelastic diffusive half-space under moving loads via Moore-Gibson-Thompson model. Othman et al. [30] discussed the influence of mechanical force on rotating thermoelastic-diffusive solid via MGT theory. Lata and Heena [31] studied the frequency domain analysis of two-dimensional transversely isotropic thermoelastic diffusive solid with two temperatures.

2. Basic equations

Following EI-Karamany and Ezzat [32], Lata and Heena [31] and Adel et al. [29], the constitutive relations are expressed as:

$$t_{ij} = \mathrm{c_{ijkl}} \mathrm{e_{kl}} - \beta_{\mathrm{ij}} T - \gamma_{\mathrm{ij}} C \,, \tag{1}$$

$$e_{ij} = \frac{1}{2}\left(u_{i,j} + u_{j,i}\right), \tag{2}$$

where $t_{ij}\left(= t_{ji}\right)$, $e_{ij}\,(= e_{ji})$, $\beta_{\mathrm{ij}}\left(= \beta_{\mathrm{ji}}\right)$ and $\gamma_{\mathrm{ij}}\left(= \gamma_{ji}\right)$ are second order tensors of stress, strain, thermal and diffusion moduli respectively, $c_{ijkl}\left(= c_{klij} = c_{jikl} = c_{jilk}\right)$ is fourth order tensor of elasticity constant, T is thermodynamic temperature, C is mass concentration, u_i is component of displacement. The comma in the subscript represents the derivative w.r.t. coordinates.

The equation of motion, based on balance of linear momentum, as also suggested by Marin et al. [33], is given as:

$$t_{ij,j} = \rho \ddot{u}_i, \tag{3}$$

where ρ denotes the mass density and the superposed dot denotes the derivative w.r.t. time.

The modified heat conduction equation based on MGT theory:

$$(1 + \tau_0)\left[\rho C^* \ddot{T} + aT_0 \ddot{C} \ + T_O \beta_{ij} \ \ddot{u}_{i,j}\right] = k_{ij}\dot{\varphi}_{,ij} + {k_{ij}}^* \varphi_{,ij} \ , \tag{4}$$

where τ_0 is thermal phase lag, C^* is specific heat at constant strain, a is measure of thermodiffusive effect, T_0 is reference temperature, φ is conductive temperature, $k_{ij}\ (= k_{ji})$, ${k_{ij}}^*\left(= {k_{ji}}^*\right)$ are second order tensors of thermal conductivity and materialistic constant respectively.

Here, two-temperature relation is given as:

$$T = \varphi - a_{ij}\varphi_{,ij}, \tag{5}$$

where a_{ij} is two-temperature parameter.

The mass diffusion equation based on the MGT theory is:

$$\left({D_{ij}}^* + D_{ij}\frac{\partial}{\partial t}\right)\left[\gamma_{ij}u_{i,j} - aT + dC\right]_{,ij} = \left(1 + \tau_1\frac{\partial}{\partial t}\right)\ddot{C}, \tag{6}$$

where a, d are measure of thermodiffusion, mass diffusion effect respectively, τ_1 denotes the diffusion relaxation time, D_{ij} (=D_{ji}) and ${D_{ij}}^*\left(= {D_{ji}}^*\right)$ are second order tensors of mass diffusion and mechano-diffusion respectively.

The chemical potential, as also discussed by Chirila and Marin [34], is related as:

$$P = -\gamma_{ij}e_{ij} + dC - aT, \tag{7}$$

Here,

$$\beta_{ij} = \beta_i\delta_{ij}, \gamma_{ij} = \gamma_i\delta_{ij}, k_{ij} = k_i\delta_{ij}, {k_{ij}}^* = {k_i}^*\delta_{ij},$$
$$D_{ij} = D_i\delta_{ij}, {D_{ij}}^* = {D_i}^*\delta_{ij}, a_{ij} = a_i\delta_{ij}, \text{(i is not summed)}.$$

3. Formulation of the problem

Consider a homogeneous, transversely isotropic thermodiffusive elastic solid occupying the half-space $z \geq 0$, where the z-axis represents the axis of material symmetry extended into the medium. The medium is initially free from any kind of mechanical, thermal and diffusive disturbances. The analysis is restricted to the xz-plane, so that each physical quantity depends upon x, z and t, i.e.,

$$\begin{gathered} u = u(x,z,t), \qquad w = w(x,z,t), \qquad v = 0, \\ T = T(x,z,t), \ C = C(x,z,t). \end{gathered} \tag{8}$$

Initial conditions:

$$\begin{gathered} u = 0, \ w = 0, \ \varphi = 0, \ C = 0, \ \dot{u} = 0, \ \dot{w} = 0, \ \dot{\varphi} = 0, \dot{C} = 0, \text{for } t = 0, z \geq 0, -\infty < x < \infty. \\ \text{Also, } u = w = \varphi = C = 0 \ for \ t > 0 \text{ when z is extremely large.} \end{gathered} \tag{9}$$

Assuming the field variables varying harmonically with time,

$$u, w, \varphi, C(x, z, t) = u, w, \varphi, C(x, z)e^{i\omega t}, \tag{10}$$

where ω is angular frequency.

Hence, the basic governing equations for this problem reduce as follow:

$$t_{xx} = c_{11}e_{xx} + c_{13}e_{zz} - \beta_1 T - \gamma_1 C, \tag{11}$$

$$t_{zz} = c_{13}e_{xx} + c_{33}e_{zz} - \beta_3 T - \gamma_3 C, \tag{12}$$

$$t_{zx} = 2c_{44}e_{xz}, \tag{13}$$

$$c_{11}\frac{\partial^2 u}{\partial x^2} + (c_{13} + c_{44})\frac{\partial^2 w}{\partial x\,\partial z} + c_{44}\frac{\partial^2 u}{\partial z^2} - \beta_1\frac{\partial}{\partial x}T - \gamma_1\frac{\partial C}{\partial x} = \rho\frac{\partial^2 u}{\partial t^2}, \tag{14}$$

$$(c_{13} + c_{44})\frac{\partial^2 u}{\partial x\,\partial z} + c_{44}\frac{\partial^2 w}{\partial x^2} + c_{33}\frac{\partial^2 w}{\partial z^2} - \beta_3\frac{\partial}{\partial z}T - \gamma_3\frac{\partial C}{\partial z} = \rho\frac{\partial^2 w}{\partial t^2}, \tag{15}$$

$$\left(k_1^{\,*} + k_1\frac{\partial}{\partial t}\right)\frac{\partial^2\varphi}{\partial x^2} + \left(k_3^{\,*} + k_3\frac{\partial}{\partial t}\right)\frac{\partial^2\varphi}{\partial z^2} = \left(1 + \tau_0\frac{\partial}{\partial t}\right)\left[\rho C^*\frac{\partial^2 T}{\partial t^2} + T_0\left(\beta_1\frac{\partial\ddot{u}}{\partial x} + \beta_2\frac{\partial\ddot{w}}{\partial z}\right) + aT_0\frac{\partial^2 C}{\partial t^2}\right], \tag{16}$$

$$\left\{\left(D_1^{\,*} + D_1\frac{\partial}{\partial t}\right)\frac{\partial^2}{\partial x^2} + \left(D_3^{\,*} + D_3\frac{\partial}{\partial t}\right)\frac{\partial^2}{\partial z^2}\right\}\left\{-\left(\gamma_1\frac{\partial u}{\partial x} + \gamma_3\frac{\partial w}{\partial z}\right) - aT + dC\right\} = \left(1 + \tau_1\frac{\partial}{\partial t}\right)\dot{C}, \tag{17}$$

$$P = -\gamma_1\frac{\partial u}{\partial x} - \gamma_3\frac{\partial w}{\partial z} + dC - aT, \tag{18}$$

here,

$$T = \varphi - \left(a_1\frac{\partial^2\varphi}{\partial x^2} + a_3\frac{\partial^2\varphi}{\partial z^2}\right), \tag{19}$$

and

$$\beta_1 = (c_{11} + c_{12})\alpha_1 + c_{13}\alpha_3,\ \beta_3 = 2c_{13}\alpha_1 + c_{33}\alpha_3,\ 2c_{66} = c_{11} - c_{12},$$
$$\gamma_1 = (c_{11} + c_{12})\hat{\alpha}_1 + c_{13}\hat{\alpha}_3, \gamma_3 = 2c_{13}\hat{\alpha}_1 + c_{33}\hat{\alpha}_3.$$

α_t and $\hat{\alpha}_t$ are the coefficients of linear thermal expansion and diffusion expansion respectively.

To reduce the complexity of problem the non-dimensional variables are introduced as following,

$$x' = \frac{x}{L},\ z' = \frac{z}{L}, u' = \frac{\rho {c_1}^2 u}{L\beta_1 T_0}, w' = \frac{\rho {c_1}^2 w}{L\beta_1 T_0}, T' = \frac{T_0}{L}, C' = \frac{C}{C_0},$$
$$t' = \frac{c_1 t}{L}, {t_{xx}}' = \frac{t_{xx}}{\beta_1 T_0}, {t_{zx}}' = \frac{t_{zx}}{\beta_1 T_0}, {a_1}' = \frac{a_1}{L^2}, {a_3}' = \frac{a_3}{L^2}, \varphi' = \frac{\varphi}{T_0}, {\tau_0}' = \frac{c_1\tau_0}{L}, {\tau_1}' = \frac{c_1\tau_1}{L}. \tag{20}$$

4. Boundary conditions

Thermal point source and chemical potential source, which are assumed to be time harmonic, are applied on the half-space ($z = 0$).

$$\begin{gathered} 1) t_{zz}(x, z, t) = 0, \\ 2)\ t_{zx}(x, z, t) = 0, \\ 3)\ \varphi(x, z, t) = \varphi_0\psi_1(x)e^{\iota\omega t}, \\ 4) P(x, z, t) = P_0\psi_2(x)e^{\iota\omega t}, \end{gathered} \tag{21}$$

where $\psi_1(x)$ is the source distribution function along $x-axis$, φ_0 is the constant temperature applied on the boundary and P_0 is the constant potential applied on the boundary.

5. Solution of the problem

After using Eq. (20) into Eqs. (14)-(17) And thereafter suppressing the primes, and then by applying Fourier transformation define

$$\hat{f}(\xi,z,s)=\int_{-\infty}^{\infty}\tilde{f}(x,z,s)e^{i\xi x}dx\,, \tag{22}$$

we obtain a system of four homogeneous equations given as following:

$$(-\xi^2+\delta_1D^2+\omega^2)\hat{u}+\iota\xi\delta_2D\hat{w}-\iota\xi\hat{T}-\iota\xi\epsilon_1\hat{C}=0\,, \tag{23}$$

$$\iota\xi\delta_2D\hat{u}+(-\xi^2\delta_1+\delta_3D^2+\omega^2)\hat{w}-\frac{\beta_3}{\beta_1}D\hat{T}-\epsilon_2D\hat{C}=0, \tag{24}$$

$$\chi_1\hat{u}+\chi_2D\hat{w}+\chi_3\hat{T}+(\Gamma_1-\Gamma_2D^2)\hat{\varphi}+\nabla_1\hat{C}=0\,, \tag{25}$$

$$(\Omega_1\xi^2-\Omega_2D^2)\iota\xi{q_1}^*\hat{u}+(\Omega_1\xi^2-\Omega_2D^2){q_2}^*D\hat{w}+(\Omega_1\xi^2-\Omega_2D^2)aT_0(1+a_1\xi^2-a_3D^2)\hat{\varphi}-dC_0(\Omega_1\xi^2-\Omega_2D^2)+\nabla_2\hat{C}=0\,, \tag{26}$$

where

$$\begin{gathered}\hat{T}=\{1-(-a_1\xi^2+a_3D^2)\}\hat{\varphi},\\ \delta_1=\frac{c_{44}}{c_{11}},\delta_2=\left(\frac{c_{13}+c_{44}}{c_{11}}\right),\delta_3=\frac{c_{33}}{c_{11}},\epsilon_1=\frac{\gamma_1C_0}{\beta_1T_0},\epsilon_2=\frac{\gamma_3C_0}{\beta_1T_0},\zeta_1=\frac{{\beta_1}^2T_0}{\rho},\zeta_2=\frac{\beta_1\beta_3T_0}{\rho}\,,{q_1}^*=\frac{\beta_1\gamma_1T_0}{\rho{c_1}^2},{q_2}^*=\frac{\beta_1\gamma_3T_0}{\rho{c_1}^2},\\ \chi_1=-(1+\tau_0\iota\omega)\zeta_1\iota\xi\omega^2,\chi_2=-(1+\tau_0\iota\omega)\zeta_2\omega^2,\chi_3=-(1+\tau_0\iota\omega)\rho C^*{c_1}^2\omega^2,\Gamma_1=\left({k_1}^*+k_1\frac{c_1}{L}\iota\omega\right)\xi^2,\Gamma_2=\left({k_3}^*+k_1\frac{c_1}{L}\iota\omega\right),\nabla_1=-(1+\tau_0\iota\omega)aC_0{c_1}^2\omega^2,\nabla_2=-(1+\tau_1\iota\omega)C_0{c_1}^2\omega^2.\end{gathered} \tag{27}$$

These resulting equations will have non-trivial solutions only if the determinant of the coefficients of $\tilde{u},\tilde{w},\tilde{\varphi}$ and $\tilde{C}$ vanishes, leading to the formation of following polynomial:

$$(d^8+\frac{Q}{P}d^6+\frac{R}{P}d^4+\frac{S}{P}d^2+\frac{T}{P})(\,\hat{u},\hat{w},\hat{\varphi},\hat{C}\,)=0. \tag{28}$$

The values of P,Q,R,S,T are listed in appendix A. The roots of the equation are of the form $\pm\lambda_i$ $(i=1,2,3,4)$. By assumption of radiation conditions $\hat{u},\hat{w},\hat{\varphi},\hat{C}$ vanish as z is extremely large. The solutions of the Eq. (28) as also discussed by Adel et al. [29] are given by:

$$\left(\hat{u},\hat{w},\hat{\varphi},\hat{C}\right)(\mu,z,s)=\sum_{j=1}^{4}(1,l_j,m_j,n_j)(A_je^{-\lambda_jz}), \tag{29}$$

where $A_j's$ are arbitrary constants, and the value of coupling constants l_j,m_j,n_j is given in appendix B.

After transforming boundary conditions into the Fourier transform domains and using the Eq. (29),

The analytic expressions for field variables are given in the Fourier domain as:

$$\hat{u}=\frac{1}{D}\sum_{i=1}^{4}(-1)^{i+1}(\varphi_0d_{2i-1}-P_0d_{2i})\,\widehat{\psi_1}(\xi)\;e^{-\lambda_iz}e^{\iota\omega t}, \tag{30}$$

$$\hat{w} = \frac{1}{D}\sum_{i=1}^{4}(-1)^{i+1} l_i(\varphi_0 d_{2i-1} - P_0 d_{2i})\widehat{\psi_1}(\xi)\, e^{-\lambda_i z} e^{\iota\omega t}, \tag{31}$$

$$\hat{\varphi} = \frac{1}{D}\sum_{i=1}^{4}(-1)^{i+1} m_i(\varphi_0 d_{2i-1} - P_0 d_{2i})\widehat{\psi_1}(\xi) e^{-\lambda_i z} e^{\iota\omega t}, \tag{32}$$

$$\hat{C} = \frac{1}{D}\sum_{i=1}^{4}(-1)^{i+1} n_i(\varphi_0 d_{2i-1} - P_0 d_{2i})\widehat{\psi_1}(\xi)\, e^{-\lambda_i z} e^{\iota\omega t}, \tag{33}$$

$$\widehat{t_{zz}} = \frac{1}{D}\sum_{i=1}^{4}(-1)^{i+1} dl_{1i}(\varphi_0 d_{2i-1} - P_0 d_{2i})\widehat{\psi_1}(\xi)\, e^{-\lambda_i z} e^{\iota\omega t}, \tag{34}$$

$$\widehat{t_{zx}} = \frac{1}{D}\sum_{i=1}^{4}(-1)^{i+1} dl_{2i}(\varphi_0 d_{2i-1} - P_0 d_{2i})\widehat{\psi_1}(\xi)\, e^{-\lambda_i z} e^{\iota\omega t}, \tag{35}$$

$$\hat{P} = \frac{1}{D}\sum_{i=1}^{4}(-1)^{i+1} dl_{4i}(\varphi_0 d_{2i-1} - P_0 d_{2i})\widehat{\psi_1}(\xi)\, e^{-\lambda_i z} e^{\iota\omega t}, \tag{36}$$

where,

The values of D, $d_i's, dl_{1i}'s$,$dl_{2i}'s$ and $dl_{4i}'s$ are given in appendix C.

6. Application

6.1 Case I: concentrated force

The solution due to application of concentrated force on the half space is derived by setting

$$\psi_1(x) = \psi_2(x) = \delta(x)\,, \tag{37}$$

where $\delta(x)$ is the dirac delta function.

Applying Fourier transformation defined by Eq. (22) on Eq. (37), we obtain

$$\widehat{\psi_1}(\xi) = \widehat{\psi_2}(\xi) = 1. \tag{38}$$

Using Eq. (38) in Eqs. (30)-(36), we obtain the components of stress, displacement, conductive temperature, mass concentration and chemical potential due to concentrated force.

6.2 Case II: Uniformly distributed force

The solution due to the application of uniformly distributed force on the half space is derived by setting

$$\{\psi_1(\mathrm{x}), \psi_2(\mathrm{x})\} = \begin{cases} 1, |x| \le a \\ 0, |x| > a \end{cases}, \tag{39}$$

Applying Fourier transformations defined by Eq. (22) on Eq. (39), we obtain

$$\{\widehat{\psi_1}(\xi), \widehat{\psi_2}(\xi)\} = \frac{2\sin(\xi a)}{\xi},\ \xi \neq 0\,, \tag{40}$$

where 2a is the non dimensional width of uniform strip load which has been applied at the origin of coordinate system (x=z=0). Using Eq. (40) in Eqs. (30)-(36), we obtain the components of stress, displacement, conductive temperature, mass concentration and chemical potential due to uniformly distributed force.

6.3 Case III: Linearly distributed force

The solution due to the application of linearly distributed force on the half space is derived by setting

$$\{\psi_1(x), \psi_2(x)\} = \begin{cases} 1 - \frac{|x|}{a}, & \text{if } |x| \le a \\ 0, & \text{if } |x| > a \end{cases}, \tag{41}$$

Applying Fourier transformation defined by Eq. (22) on Eq. (41), we obtain

$$\{\widehat{\psi_1}(\xi), \widehat{\psi_2}(\xi)\} = \frac{2[1-cos(\xi\, a)]}{\xi^2 a}, \tag{42}$$

where 2a is the non dimensional width of strip load which has been applied at the origin of coordinate system (x=z=0). Using Eq. (41) in Eqs. (30)-(36), we obtain the components of stress, displacement, conductive temperature, mass concentration and chemical potential due to linearly distributed force.

7. Particular cases

1. By keeping $a = d = \gamma_{ij} = 0$, we can get the results without the effect of diffusion.
2. By keeping $a_1 = a_3 = 0$, we can have the results without two-temperature thermoelastic diffusion problem.

8. Inversion of the Fourier transform

To get the solution back in the physical domain, inversion technique for Fourier transform as employed by Lata [35] and Lata and Heena [36] has been employed as follow:

$$f(x, z, \omega) = \frac{1}{2\pi}\int_{-\infty}^{\infty} e^{-\iota\xi x}\, \hat{f}(\xi, z, \omega) d\xi = \frac{1}{\pi}\int_{0}^{\infty} (\cos(\xi x)\, \widehat{f_i} - \sin(\xi x)\, \widehat{f_{ii}} d\xi, \tag{43}$$

where f_i and f_{ii} are, respectively, the even and odd parts of the function $\hat{f}(\xi, z, \omega)$. Romberg integration with adaptive size, as described in Press et al. [37], was employed to evaluate the integral in Eq. (45). This method builds on successive refinements of the extended trapezoidal rule followed by extrapolation of the results to the limit when the step size approaches zero.

9. Numerical results and discussions

Following Dhaliwal and Singh [38], Lata and Heena [31] and Adel et al. [29] copper material is taken for graphical representation,

$$c_{11} = 18.78 \times 10^{10}\ \text{Kgm}^{-1}\text{s}^{-2},$$
$$c_{12} = 8.76 \times 10^{10}\ \text{Kgm}^{-1}\text{s}^{-2},$$
$$c_{13} = 8.0 \times 10^{10}\ \text{Kgm}^{-1}\text{s}^{-2},$$
$$c_{33} = 17.2 \times 10^{10}\ \text{Kgm}^{-1}\text{s}^{-2},$$
$$c_{44} = 5.06 \times 10^{10}\ \text{Kgm}^{-1}\text{s}^{-2},$$
$$\alpha_1 = 2.98 \times 10^{-5}\ \text{K}^{-1},\ \alpha_3 = 2.4 \times 10^{-5}\ \text{K}^{-1},$$
$$\widehat{\alpha_1} = 2.1 \times 10^{-4} m^3 Kg^{-1},$$

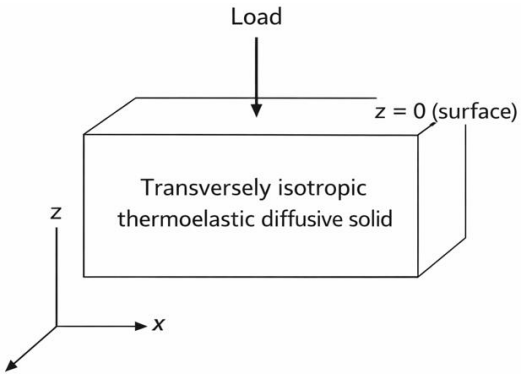

Figure 1. Geometry of the problem

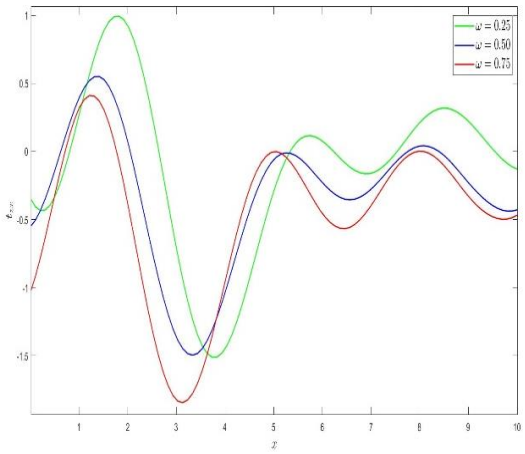

Figure 2. Variation of tangential stress t_{zx} w.r.t. distance x (concentrated load)

$$\hat{\alpha}_3 = 2.5 \times 10^{-4}\ \mathrm{m^3 Kg^{-1}}, \qquad T_0 = 0.293 \times 10^3\ \mathrm{K},$$
$$C^* = 0.6331 \times 10^3\ \mathrm{JKg^{-1}K^{-1}},$$
$$a = 2.4 \times 10^4\ \mathrm{m^2 s^{-2} K^{-1}}, d = 13 \times 10^5\ \mathrm{m^2 s^{-2} K^{-1}},$$
$$\rho = 8.954 \times 10^3\ \mathrm{Kg\,m^{-3}}$$
$$k_1 = 0.433 \times 10^3\ \mathrm{Wm^{-1}K^{-1}},$$
$$k_3 = 0.450 \times 10^3\ \mathrm{Wm^{-1}K^{-1}},$$
$$k_1^* = 0.02 \times 10^3\ \mathrm{Nsec^{-2}K^{-1}},$$
$$k_3^* = 0.04 \times 10^3\ \mathrm{Nsec^{-2}K^{-1}},$$

Numerical simulations are conducted on the plane $z = 0.5$ at $t = 0.5$. The other parameters are taken as $D_1 = 0.95$, $D_3 = 0.90$, ${D_1}^* = 0.85$, ${D_3}^* = 0.80$, $\tau_0 = 0.03, \tau_1 = 0.02$, $P_0 = \varphi_0 = 2$, $C_0 = 2, a_1 = 0.04, a_3 = 0.06$ in dimensionless form. Figs. 1-12 represent the variation of stress components, conductive temperature and chemical potential w.r.t under three different kind of loads.

- The green solid curve corresponds to $\omega = 0.25$.
- The blue solid curve corresponds to $\omega = 0.50$.
- The red solid curve corresponds to $\omega = 0.75$.

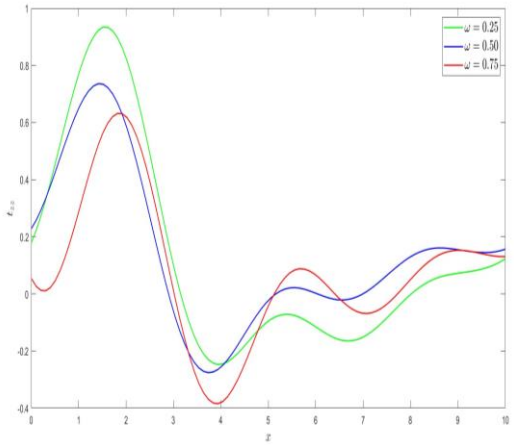

Figure 3. Variation of normal stress t_{zz} w.r.t. distance x (concentrated load)

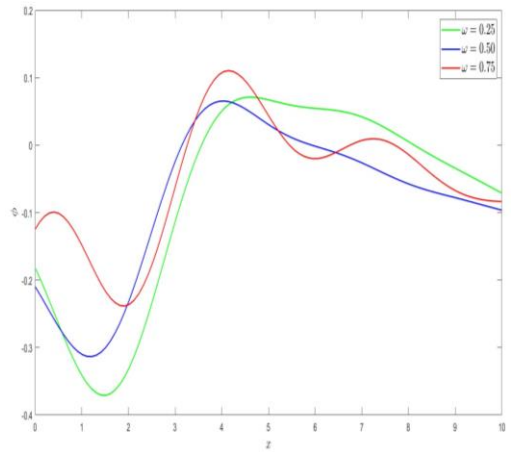

Figure 4. Variation of conductive temperature φ w.r.t. distance x (concentrated load)

Fig. 2 represents the variation of stress component w.r.t. distance x for different values of harmonic frequency. Clearly, t_{zx} represents the oscillatory behavior in all the three cases of ω, Near $x = 0$, the stress component exhibits a sharp negative value for all the considered values of ω. The strong initial effect occurs because the applied concentrated thermal and chemical potential load produces an immediate mechanical deformation, followed by alternating rises and falls as the distances increases. For $\omega = 0.25$, the stress component t_{zx} shows the broader peaks and troughs with comparatively larger amplitude. A reduction in amplitude is observed with increasing ω. As ω increases, the oscillations become more compact and frequent. In all the three cases, t_{zx} attains its maximum magnitude near $x = 2$, while the minimum magnitude appears around $x = 3$. Beyond $x = 3$, the oscillatory pattern remains persistent. It is clear from Fig. 3, for all the considered values of ω, t_{zz} increases from its initial value near $x = 0$, and attains its maximum magnitude around $x = 2$. As x increases further, a decline in values of stress component t_{zz} can be seen, and it reaches its lowest value near $x = 4$ for all the considered cases. Beyond this the alternating pattern is persistent through out the domain. A clear influence of ω is visible. As ω

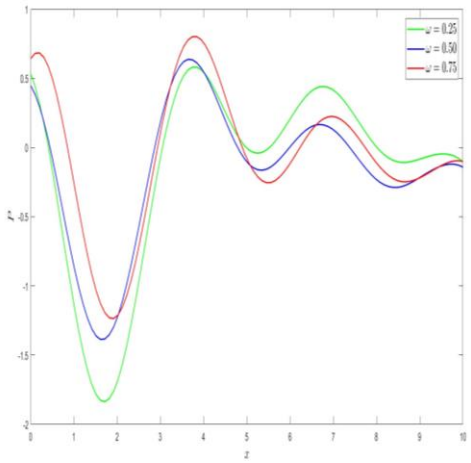

Figure 5. Variation of chemical potential P w.r.t. distance x (concentrated load)

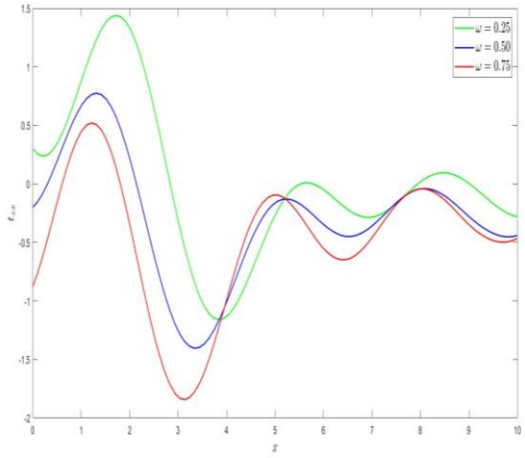

Figure 6. Variation of tangential stress t_{zx} w.r.t. distance x (uniformly distributed load)

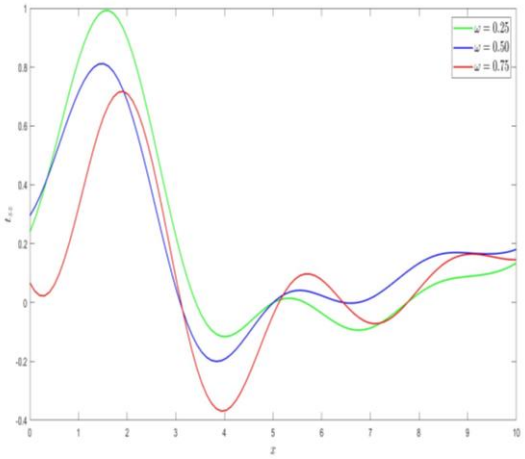

Figure 7. Variation of normal stress t_{zz} w.r.t. distance x (uniformly distributed load)

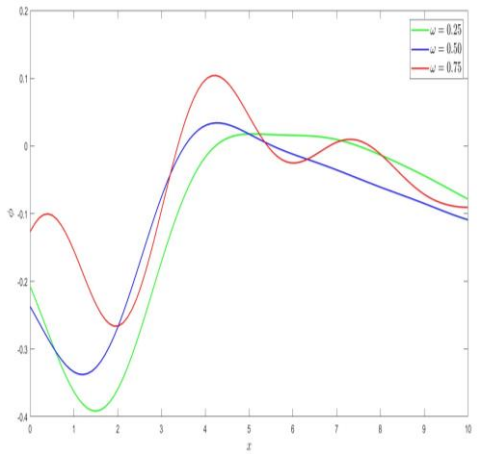

Figure 8. Variation of conductive temperature φ w.r.t. distance x (uniformly distributed load)

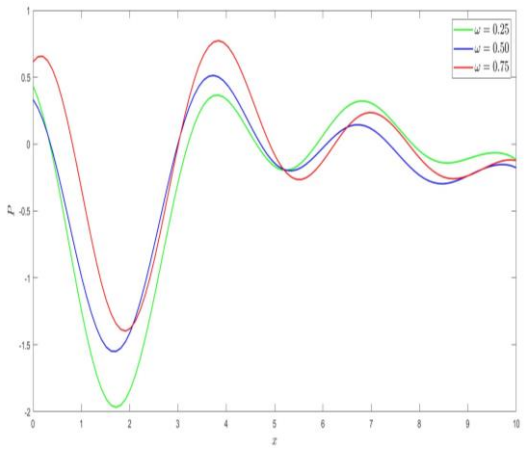

Figure 9. Variation of chemical potential P w.r.t. distance x (uniformly distributed load)

increases, the spacing between successive peaks decreases, and the amplitude of oscillations reduce significantly.

From Fig. 4, it can be seen that φ decreases immediately from its initial value and attains its minimum near $x = 2$. After $x = 2$, it starts increasing for the three cases of ω, and attains its maximum around $x = 4$. Beyond $x = 5$, the curves corresponding to $\omega = 0.25$ and $\omega = 0.50$ exhibit nearly negligible variations. In contrast, the curve for $\omega = 0.75$ continues to show small yet noticeable oscillations. The oscillatory pattern for P w.r.t. distance x can be observed from Fig. 5. The chemical potential P shows an initial decline in its values for all the considered cases of ω and attained its minimum value nearly $x = 2$. After $x = 2$, all the three curves show increase in values of P and it attains it maximum value nearly $x = 4$. After $x = 5$, smaller oscillations are observed for all the values of ω. P assumes its lowest value for $\omega = 0.25$ and highest value for $\omega = 0.75$.

Figs. 6-9 represent the variation in tangential stress t_{zx}, normal stress t_{zz}, conductive temperature φ and chemical potential P w.r.t. distance x due to uniformly distributed load. The

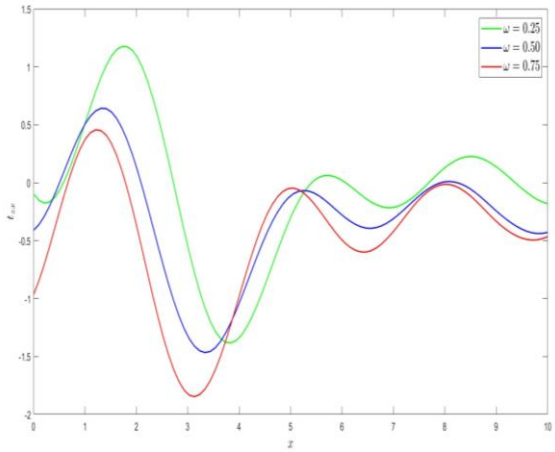

Figure 10. Variation of tangential stress t_{zx} w.r.t. distance x (linearly distributed load)

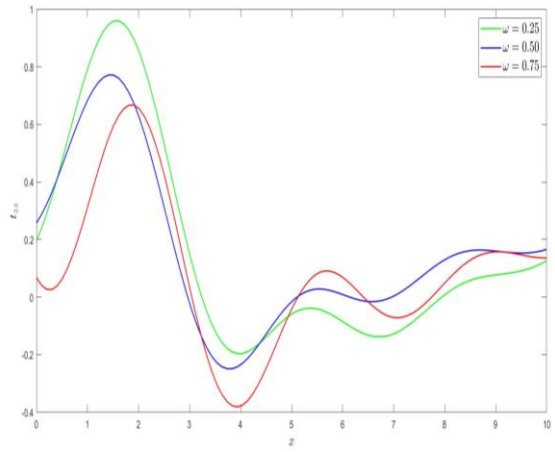

Figure 11. Variation of normal stress t_{zz} w.r.t. distance x (linearly distributed load)

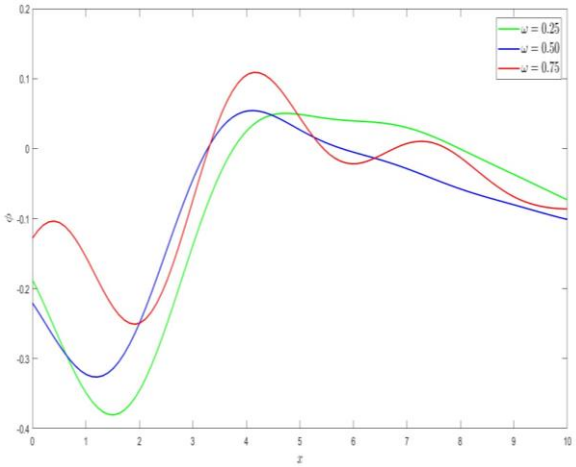

Figure 12. Variation of conductive temperature φ w.r.t. distance x (linearly distributed load)

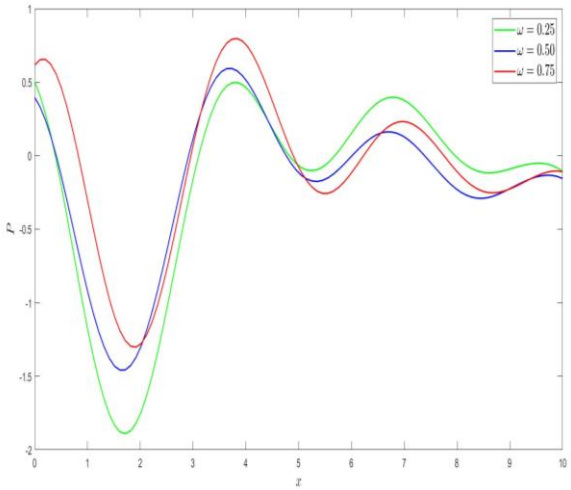

Figure 13. Variation of chemical potential P w.r.t. distance x (linearly distributed load)

same kind of oscillatory pattern in curves is observed as in case of concentrated load, the only difference is in magnitude which is due to different load application.

Figs. 10-13 represent the variation in tangential stress t_{zx}, normal stress t_{zz}, conductive temperature φ and chemical potential P w.r.t. distance x due to linearly distributed load, which exhibit the same kind of oscillatory behavior as observed in other two kinds of loading.

10. Conclusions

In this research, the thermoelastic diffusive response of transversely isotropic material under chemical potential and thermal loads has been observed. MGT theory of thermoelasticity has been considered to discuss the behavior of field variables which are assumed to be varying harmonically with time. The oscillatory behavior of stress components, conductive temperature and chemical potential has been observed w.r.t. distance x. The effect of ω on field variables has been determined by taking different values of ω. As ω increases, the oscillations become frequent and compact, indicating that field variables oscillate at shorter wavelengths at higher values of ω. This systematic reduction in amplitude and tightening of oscillations with increasing frequency reflects the frequency-dependent dispersive behavior of the MGT model, where the presence of relaxation parameters leads to stronger damping of higher-frequency responses.

References

1. Biot, M.A. (1956). Thermoelasticity and irreversible thermodynamics. Journal of Applied Physics, 27(3), 240-253. https://doi.org/10.1063/1.1722351.
2. Lord, H.W. and Shulman, Y. (1967). A generalized dynamical theory of thermoelasticity. Journal of the Mechanics and Physics of Solids, 15(5), 299-309. https://doi.org/10.1016/0022-5096(67)90024-5.
3. Green, A.E. and Lindsay, K. (1972). Thermoelasticity. Journal of Elasticity, 2(1), 1-7. https://doi.org/10.1007/BF00045689.

4. Green, A.E. and Naghdi, P.M. (1991). A re-examination of basic postulates of thermomechanics. Proceedings of the Royal Society A: Mathematical, Physical and Engineering Sciences, 432(1885), 171-194. https://doi.org/10.1098/rspa.1991.0012.
5. Green, A.E. and Naghdi, P.M. (1992). On undamped heat waves in an elastic solid. Journal of Thermal Stresses, 15, 253-264. http://doi.org/10.1080/01495739208946136.
6. Green, A.E. and Naghdi, P.M. (1993). Thermoelasticity without energy dissipation. Journal of Elasticity, 31, 189-208. https://doi.org/10.1007/BF00044969.
7. Tzou, D.Y. (1995). A unified approach for heat conduction from macro-to micro-scales. Journal of Heat Transfer, 117(1), 8-16. https://doi.org/10.1115/1.2822329.
8. Choudhary, S.K.R. (2007). On a thermoelastic three-phase lag model. Journal of Thermal Stresses, 30(3), 231-238. https://doi.org/10.1080/01495730601130919.
9. Thompson, P.A. (1972). Compressible-fluid dynamics. MCGraw-Hill, USA.
10. Dell'Oro, F. and Pata, V. (2017). On the Moore-Gibson-Thompson equation and its relation to linear viscoelasticity. Applied Mathematics and Optimization, 76(4), 641-655. https://doi.org/10.1007/s00245-016-9365-1.
11. Quintanilla, R. (2019). Moore-Gibson-Thompson thermoelasticity. Mathematics and Mechanics of Solids, 24(12), 4020-4037. https://doi.org/10.1177/1081286519862007.
12. Quintanilla, R. (2020). Moore-Gibson-Thompson thermoelasticity with two temperatures. Applications in Engineering Science, 1, 100006. https://doi.org/10.1016/j.apples.2020.100006.
13. Nowacki, W. (1974). Dynamic problems of thermodiffusion in solids. Bulletin of the Polish Academy of Sciences: Technical Sciences, 22, 55-64.
14. Nowacki, W. (1974). Dynamic problems of thermodiffusion in solids II. Bulletin of the Polish Academy of Sciences: Technical Sciences, 22, 129-135.
15. Nowacki, W. (1974). Dynamic problems of thermodiffusion in solids III. Bulletin of the Polish Academy of Sciences: Technical Sciences, 22, 257-266.
16. Sherief, H.H., Hamza, F.A., Saleh, H.A. (2004). The theory of generalized thermoelastic diffusion. International Journal of Engineering Science, 42(5-6), 591-608. https://doi.org/10.1016/j.ijengsci.2003.05.001.
17. Sharma, N., Kumar, R., Ram, P. (2008). Dynamical behavior of generalized thermoelastic diffusion with two relaxation times in frequency domain. Structural Engineering and Mechanics, 28(1), 19-38. https://doi.org/10.12989/sem.2008.28.1.019.
18. Abbas, I.A., Kumar, R., Chawla, V. (2012). Response of thermal source in a transversely isotropic thermoelastic half-space with mass diffusion by using a finite element method. Chinese Physics B, 21, 084601. http://doi.org/10.1088/1674-1056/21/8/084601.
19. Abbas, I.A., Othman, M.I.A. (2012). Plane waves in generalized thermo-microstretch elastic solid with thermal relaxation using finite element method. International Journal of Thermophysics, 33, 2407-2423. http://doi.org/10.1007/s10765-012-1340-8.
20. Kumar, R., Gupta, V., Abbas, I.A. (2013). Plane deformation due to thermal source in fractional order thermoelastic media. Journal of Computational and Theoretical Nanoscience, 10, 2520-2525. http://doi.org/10.1166/jctn.2013.3241.
21. Zenkour, A. (2014). Two-temperature generalized thermoelastic interaction in an infinite fiber-reinforced anisotropic plate containing a circular cavity with two relaxation times. Journal of Computational and Theoretical Nanoscience, 11(1), 1-7. http://doi.org/10.1166/jctn.2014.3309.
22. Abbas, I.A., Abo-Dahab, S.M. (2014). On the numerical solution of thermal shock problem for generalized magneto-thermoelasticity for an infinitely long annular cylinder with variable thermal conductivity. Journal of Computational and Theoretical Nanoscience, 11(3), 607-618. http://doi.org/10.1166/jctn.2014.3402.
23. Abouelregal, A.E. and Sedighi, H.M. (2021). A new insight into the interaction of thermoelasticity with mass diffusion for a half-space in the context of Moore-Gibson-Thompson thermodiffusion theory. Applied Physics A: Material Science and Processing, 127, 582. https://doi.org/10.1007/s00339-021-04725-0.

24. Sur, A. (2023). Moore-Gibson-Thompson generalized heat conduction in a thick plate. Indian Journal of Physics, 98(5), 1715-1726. https://doi.org/10.1007/s12648-023-02931-5.
25. Abouelregal, A.E., Askar, S.S., Marin, M., Mohamed, B. (2023). The theory of thermoelasticity with a memory-dependent dynamic response for a thermo-piezoelectric functionally graded rotating rod. Scientific Reports, 13(1), 9052. https://doi.org/10.1038/s41598-023-36371-2.
26. Abouelregal, A.E., Marin, M., Öchsner, A. (2023). The influence of a non-local Moore-Gibson-Thompson heat transfer model on an underlying thermoelastic material under the model of memory-dependent derivatives. Continuum Mechanics and Thermodynamics, 35(2), 1-18. https://doi.org/10.3390/sym12020321.
27. Singh, S., Lata, P. (2024). Time harmonic interactions in a nonlocal isotropic thermoelastic thick circular plate without energy dissipation. Advances in Materials Research, 13(5), 417-429. https://doi.org/10.12989/amr.2024.13.5.417.
28. Gerba, B.F., Lata, P., Singh, S.B. (2025). Interactions in a nonlocal isotropic thermoelastic solid with diffusion due to thermal source in frequency domain. Coupled Systems Mechanics, 14(4), 313-325. https://doi.org/10.12989/csm.2025.14.4.313.
29. Adel, M., Sharma, R., Kumar, R. Sharma, P.K., Mahdy, A.M.S., Lotfy, K. (2025). Thermoelastic-diffusive response of half-space under moving loads via Moore-Gibson-Thompson model. International Communication in Heat and Mass transfer, 166, 109226. https://doi.org/10.1016/j.icheatmasstransfer.2025.109226.
30. Othman, M.I.A., Said, S.M., Fathy, R.A., Eldemerdash, M.G. (2025). Effect of mechanical force on a rotating diffusive-thermoelastic solid with microconcentration via Moore-Gibson-Thompson theory. International Communications in Heat and Mass Transfer, 162, 108597. https://doi.org/10.1016/j.icheatmasstransfer.2025.108597.
31. Lata, P., Heena. (2025). Frequency-domain analysis of transversely isotropic thermoelastic diffusive solid with two-temperature. Advances in Material Research, 14(5), 429-448. https://doi.org/10.12989/amr.2025.14.5.429.
32. EI-Karamany, A.S., Ezzat, M.A. (2016). Thermoelastic diffusion with memory-dependent derivative. Journal of Thermal Stresses, 39(9), 1035-1050. https://doi.org/10.1080/01495739.2016.1192847.
33. Marin, M., Agarwal, R.P., Abbas, I.A. (2014). Effect of intrinsic rotations, microstructural expansion and contractions in initial boundary value problem of thermoelastic bodies. Boundary Value Problems, 2014(1), 129. https://doi.org/10.1186/1687-2770-2014-129.
34. Chirila, A., Marin, M. (2021). Wave propagation in diffusive microstretch thermoelasticity. Mathematics and Computers in Simulations, 189, 99-113. https://doi.org/10.1016/j.matcom.2020.08.012.
35. Lata, P. (2019). Time harmonic interactions in fractional thermoelastic diffusive thick circular plate. Coupled Systems Mechanics, 8(1), 39-53. https://doi.org/10.12989/csm.2019.8.1.039.
36. Lata, P., Heena (2024). Thermomechanical interactions in a transversely isotropic thermoelastic media with diffusion due to inclined load. Structural Engineering and Mechanics, 90(3), 263-272. https://doi.org/10.12989/sem.2024.90.3.263.
37. Press, W.H., Teukolsky, S.A., Vellerling, W.T., Flannery, B.P. (1986). Numerical recipes in fortran. Cambridge University Press, Cambridge.
38. Dhaliwal, R., Singh, A. (1980). Dynamic coupled thermoelasticity. Hindustan Publication Corporation, New Delhi.

Appendix A

The values of P, Q, R, S, T are given as:

$$P = \delta_1(-\delta_3 G_{11} - r_8 G_{12} - \epsilon_2 G_{16}),$$

$$Q = -(\xi^2 - \omega^2)(-\delta_3 G_{11} - r_8 G_{12} - \epsilon_2 G_{16}) + \delta_1(\delta_3 G_4 + r_6 G_{11} - r_7 G_{12} - r_8 G_5 - \epsilon_2 G_{13}) + \iota\xi\delta_2(\iota\xi\delta_2 G_{11} + r_8 G_7 + \epsilon_2 G_{14}) + r_5(-\delta_3 G_7 - \epsilon_2 G_{10} + \iota\xi\delta_2 G_{12}) + \epsilon_1\iota\xi(\iota\xi\delta_2 G_{16} - \delta_3 G_{14} + r_8 G_{10}),$$

$$R = \delta_1(\delta_3 G_1 - r_6 G_4 - r_7 G_5 - \epsilon_2 G_6) - (\xi^2 - \omega^2)(\delta_3 G_6 + r_6 G_{11} - r_7 G_{12} - r_8 G_5 - \epsilon_2 G_{13}) - \iota\xi\delta_2(\iota\xi\delta_2 G_4 - r_7 G_7 - r_8 G_2 - \epsilon_2 G_9) + r_4(-\delta_3 G_7 - \epsilon_2 G_{10} + \iota\xi\delta_2 G_{12}) + r_5(\iota\xi\delta_2 G_5 - \delta_3 G_2 + r_6 G_7 - \epsilon_2 G_8) + \epsilon_1\iota\xi(\iota\xi\delta_2 G_{13} - \delta_3 G_9 + r_6 G_{14} + r_7 G_{15} + r_8 G_8),$$

$$S = -\delta_1 r_6 G_1 - (\xi^2 - \omega^2)(\delta_3 G_1 - r_6 G_4 - r_7 G_5 - \epsilon_2 G_6) - \iota\xi\delta_2(\iota\xi\delta_2 G_1 - r_7 G_2 - \epsilon_2 G_3) + r_5 r_6 G_2 + r_4(\iota\xi\delta_2 G_5 - \delta_3 G_2 + r_6 G_7 - \epsilon_2 G_8) + \iota\xi\epsilon_1(\iota\xi\delta_2 G_6 - \delta_3 G_3 + r_6 G_9 - r_7 G_8),$$

$$T = (\xi^2 - \omega^2) r_6 G_1 + r_4 r_6 G_2 + \iota\xi\epsilon_1 r_6 G_3,$$

where,

$$G_1 = r_9 r_{15} - \nabla_1 r_1, G_2 = \chi_1 r_{15} - \nabla_1 r_{11},$$
$$G_3 = \chi_1 r_1 - r_9 r_{11}, G_4 = r_9 r_{16} - r_{10} r_{15} + \nabla_1 r_2,$$
$$G_5 = \chi_2 r_{15} - \nabla_1 r_{13}, G_6 = \chi_2 r_1 - r_9 r_{13},$$
$$G_7 = \chi_1 r_{16} - \nabla_1 r_{12}, G_8 = \chi_1 r_{13} - \chi_2 r_{11},$$
$$G_9 = -\chi_1 r_2 + r_9 r_{12} + r_{10} r_{11}, G_{10} = \chi_1 r_{14} + \chi_2 r_{12},$$
$$G_{11} = r_{10} r_{16} + \nabla_1 r_3, G_{12} = \chi_2 r_{16} - \nabla_1 r_{14},$$
$$G_{13} = -\chi_2 r_2 - r_9 r_{14} + r_{10} r_{13}, G_{14} = \chi_1 r_3 - r_{10} r_{12},$$
$$G_{15} = \chi_2 r_{12} + \chi_1 r_{14}, G_{16} = \chi_2 r_3 + r_{10} r_{14},$$
$$r_1 = a T_0 \Omega_1 \xi^2 (1 + a_1 \xi^2),$$
$$r_2 = a T_0 \Omega_2 (1 + a_1 \xi^2) + a T_0 \Omega_1 a_3,$$
$$r_3 = a T_0 \Omega_2 a_3, r_4 = -\iota\xi(1 + a_1 \xi^2),$$
$$r_5 = a_3 \iota\xi, r_6 = \xi^2 \delta_1 - \omega^2, r_7 = -\frac{\beta_3}{\beta_1}(1 + a_1 \xi^2),$$
$$r_8 = \frac{\beta_3}{\beta_1} a_3, r_9 = \chi_3 (1 + a_1 \xi^2) + \Gamma_1,$$
$$r_{10} = \chi_3 a_3 + \Gamma_2,$$
$$r_{11} = \iota\Omega_1 \xi^3 q_1^*, r_{12} = \iota\Omega_2 \xi q_1^*, r_{13} = \Omega_1 \xi^2 q_2^*,$$
$$r_{14} = -\Omega_2 q_2^*, r_{15} = -d C_0 \Omega_1 \xi^2 - \nabla_2, r_{16} = d C_0 \Omega_2.$$

Appendix B

The values of coupling constants are given as:

$$l_i = \frac{b_5 \lambda_i^5 + b_6 \lambda_i^3 + b_7 \lambda_i}{b_1 \lambda_i^6 + b_2 \lambda_i^4 + b_3 \lambda_i^2 + b_4},$$

$$m_i = \frac{b_8 \lambda_i^4 + b_9 \lambda_i^2 + b_{10}}{b_1 \lambda_i^6 + b_2 \lambda_i^4 + b_3 \lambda_i^2 + b_4},$$

$$n_i = \frac{b_{11}\lambda_i^6 + b_{12}\lambda_i^4 + b_{13}\lambda_i^2 + b_{14}}{b_1\lambda_i^6 + b_2\lambda_i^4 + b_3\lambda_i^2 + b_4}\,, (i = 1,2,3,4)$$

where,

$$b_1 = -\delta_3 G_{11} - r_8 G_{12} - \epsilon_2 G_{16},$$
$$b_2 = \delta_3 G_4 + r_6 G_{11} - r_7 G_{12} - r_8 G_5 - \epsilon_2 G_{13},$$
$$b_3 = \delta_3 G_1 - r_6 G_4 - r_7 G_5 - \epsilon_2 G_6, b_4 = r_6 G_1,$$
$$b_5 = -\iota\xi\delta_2 G_{11} - r_8 G_7 - \epsilon_2 G_{14},$$
$$b_6 = \iota\xi\delta_2 G_4 - r_7 G_7 - r_8 G_2 - \epsilon_2 G_9,$$
$$b_7 = \iota\xi\delta_2 G_1 - r_7 G_2 - \epsilon_2 G_3,$$
$$b_8 = -\delta_3 G_7 - \epsilon_2 G_{10} + \iota\xi\delta_2 G_{12},$$
$$b_9 = \iota\xi\delta_2 G_5 - \delta_3 G_2 + r_6 G_7 - \epsilon_2 G_8,$$
$$b_{10} = r_6 G_2,$$
$$b_{11} = \iota\xi\delta_2 G_{15} - \delta_3 G_{14} + r_8 G_{10},$$
$$b_{12} = \iota\xi\delta_2 G_{13} - \delta_3 G_9 + r_6 G_{14} + r_7 G_{10} + r_8 G_8,$$
$$b_{13} = \iota\xi\delta_2 G_6 - \delta_3 G_3 + r_6 G_9 + r_7 G_8,$$
$$b_{14} = r_6 G_3,$$

Appendix C

$$D = dl_{11}det_1 - dl_{12}det_2 + dl_{13}det_3 - dl_{14}det_4,$$

where,

$$det_1 = dl_{22}(dl_{33}dl_{44} - dl_{34}dl_{43}) - dl_{23}(dl_{32}dl_{44} - dl_{34}dl_{42}) + dl_{24}(dl_{32}dl_{43} - dl_{33}dl_{42}),$$
$$det_2 = dl_{21}(dl_{33}dl_{44} - dl_{34}dl_{43}) - dl_{23}(dl_{31}dl_{44} - dl_{34}dl_{41}) + dl_{24}(dl_{31}dl_{43} - dl_{33}dl_{41}),$$
$$det_3 = dl_{21}(dl_{32}dl_{44} - dl_{34}dl_{42}) - dl_{22}(dl_{31}dl_{44} - dl_{34}dl_{41}) + dl_{24}(dl_{31}dl_{42} - dl_{32}dl_{41}),$$
$$det_4 = dl_{21}(dl_{32}dl_{43} - dl_{33}dl_{42}) - dl_{22}(dl_{31}dl_{43} - dl_{33}dl_{41}) + dl_{23}(dl_{31}dl_{42} - dl_{32}dl_{41}),$$

$$d_1 = dl_{12}P_{21} - dl_{13}P_{22} + dl_{14}P_{23},$$
$$d_2 = dl_{12}P_{24} - dl_{13}P_{25} + dl_{14}P_{26},$$
$$d_3 = dl_{11}P_{21} - dl_{13}P_{27} + dl_{14}P_{28},$$
$$d_4 = dl_{11}P_{24} - dl_{13}P_{29} + dl_{14}P_{30},$$
$$d_5 = dl_{11}P_{22} - dl_{12}P_{27} + dl_{14}P_{31},$$
$$d_6 = dl_{11}P_{25} - dl_{12}P_{29} + dl_{14}P_{32}$$
$$d_7 = dl_{11}P_{23} - dl_{12}P_{28} + dl_{13}P_{31},$$
$$d_8 = dl_{11}P_{26} - dl_{12}P_{30} + dl_{13}P_{32},$$

$$P_{21} = dl_{23}dl_{44} - dl_{43}dl_{24},$$
$$P_{22} = dl_{22}dl_{44} - dl_{42}dl_{24},$$
$$P_{23} = dl_{22}dl_{43} - dl_{23}dl_{42},$$
$$P_{24} = dl_{23}dl_{34} - dl_{24}dl_{33},$$
$$P_{25} = dl_{22}dl_{34} - dl_{24}dl_{32},$$
$$P_{26} = dl_{22}dl_{33} - dl_{23}dl_{32},$$
$$P_{27} = dl_{21}dl_{44} - dl_{24}dl_{41},$$
$$P_{28} = dl_{21}dl_{43} - dl_{23}dl_{41},$$

$$P_{29} = dl_{21}dl_{34} - dl_{24}dl_{31},$$
$$P_{30} = dl_{21}dl_{33} - dl_{23}dl_{31},$$
$$P_{31} = dl_{21}dl_{42} - dl_{22}dl_{41},$$
$$P_{32} = dl_{21}dl_{32} - dl_{22}dl_{31},$$

where,

$$dl_{1i} = \frac{i\xi c_{13} - \lambda_i l_i c_{33}}{c_{11}} - \frac{\beta_3 m_i\left(1 + a_1\xi^2 - a_3\lambda_i^2\right)}{\beta_1} - \frac{\gamma_3 n_i C_o}{\beta_1 T_o},$$

$$dl_{2i} = -\frac{c_{44}}{c_{11}}(\lambda_i - \iota\xi l_i),$$

$$dl_{3i} = m_i,$$

$$dl_{4i} = -\frac{\beta_1 T_0}{c_{11}}\iota\xi + \frac{\gamma_3}{\gamma_1}\frac{\beta_1 T_0}{c_{11}}\lambda_i l_i + \frac{d}{\gamma_1}n_i C_0 - \frac{a}{\gamma_1}T_0 m_2\left(1 + a_1\xi^2 - a_3\lambda_i^2\right), \text{ for } i = 1,2,3,4$$